Poly(vinyl alcohol) cryogel phantoms for use in ultrasound and MR imaging

To cite this article: K J M Surry *et al* 2004 *Phys. Med. Biol.* **49** 5529

View the article online for updates and enhancements.

Poly(vinyl alcohol) cryogel phantoms for use in ultrasound and MR imaging

K J M Surry[1,2]**, H J B Austin**[1]**, A Fenster**[1,2,3] **and T M Peters**[1,2,3]

[1] Imaging Research Laboratories, Robarts Research Institute, London, Canada
[2] Department of Medical Biophysics, University of Western Ontario, London, Canada
[3] Department of Diagnostic Radiology and Nuclear Medicine, University of Western Ontario, London, Canada

E-mail: tpeters@imaging.robarts.ca

Abstract

Poly(vinyl alcohol) cryogel, PVA-C, is presented as a tissue-mimicking material, suitable for application in magnetic resonance (MR) imaging and ultrasound imaging. A 10% by weight poly(vinyl alcohol) in water solution was used to form PVA-C, which is solidified through a freeze–thaw process. The number of freeze–thaw cycles affects the properties of the material. The ultrasound and MR imaging characteristics were investigated using cylindrical samples of PVA-C. The speed of sound was found to range from 1520 to 1540 m s^{-1}, and the attenuation coefficients were in the range of 0.075–0.28 dB (cm MHz)$^{-1}$. T1 and T2 relaxation values were found to be 718–1034 ms and 108–175 ms, respectively. We also present applications of this material in an anthropomorphic brain phantom, a multi-volume stenosed vessel phantom and breast biopsy phantoms. Some suggestions are made for how best to handle this material in the phantom design and development process.

Introduction

Poly(vinyl alcohol) cryogel (PVA-C) has been introduced as a medical imaging phantom material in magnetic resonance imaging (MRI) by Mano *et al* (1986) and by Chu and Rutt (1997). Poly(vinyl alcohol) (PVA) is a widely used, non-toxic, industrial compound, often employed in glue in food packaging or for children's craft projects (Dyson 1998). However, by using the appropriate PVA and water solution, this material can be easily formed into a gel possessing tissue-mimicking properties.

PVA is derived from the hydrolysis of poly(vinyl acetate) which is a process that never goes to completion, resulting in a final product that is a mixture of PVA and poly(vinyl acetate). The published grade of the PVA refers to its purity. An aqueous solution of high-grade PVA can

be gelled into a cross-linked hydrogel by the formation of crystallites during repeated freeze–thaw cycles (Stauffer and Peppas 1992, Peppas 1975). The number of crystallites formed, the resulting rigidity and several other properties, are affected by the number of freeze–thaw cycles, the freeze time, the thaw time and the concentration of PVA in the aqueous solution (Hassan and Peppas 2000, Mori *et al* 1997, Nagura *et al* 1989). It is this process of gelation by freezing to $-20\,^{\circ}C$ that has led to the descriptor of poly(vinyl alcohol) *cryogel*. The purpose of this paper is to present examples of the use of PVA-C in our research as a phantom material for imaging studies, rather than to explore the chemical nature of this material. Information on the chemistry of PVA-C can be found in several sources (Cha *et al* 1993, Hassan and Peppas 2000, Lozinsky *et al* 1986, Nagura *et al* 1984, Watase 1989).

Historically, tissue-mimicking materials (TMMs) have most commonly been made with an agar or gelatin base (Blechinger *et al* 1988, De Korte *et al* 1997, Madsen *et al* 1978, Mitchell *et al* 1986, Rickey *et al* 1995, Ryan and Foster 1997). Our incentives for developing an alternative approach were both to develop higher strength vascular models and also to produce multi-component, multi-modal phantoms. It is also possible to prescribe the mechanical properties of PVA-C to some extent, allowing phantoms to be produced with 'realistic' tactility and mechanical properties. It has also been shown that this material can be used in thermal and radiation dosimetry applications. These two features have been published separately (Lukas *et al* 2001, Chu *et al* 2000).

Phantoms are used in medical imaging research to substitute for real tissue in studies where *in vivo* models are inappropriate. Phantoms can be modelled on anatomical features, such as vessels and vascular trees, including structures such as white and grey matter and lesions, or mechanical structures that behave appropriately, such as a pulsating vessel wall. One benefit to modelling these features with PVA-C rather than using anatomical specimens is the phantom can be made precisely, with a known structure that is used as 'truth'. This is particularly useful for segmentation algorithm development where the digitally segmented structure must be compared to a known geometry.

Other benefits to phantom use include their long-term structural stability, the ease of registering multiple phantom images to one another in subsequent studies, the ability to perform long imaging procedures without concern for subject motion or discomfort and also to test and develop novel medical procedures. As we demonstrate below, PVA-C is an ideal material in all of these situations. Also, phantoms usually have a simpler structure than anatomical models. This allows for a simplification of the problem, by restricting the number of experimental variables. The structure can be focused to a specific problem, or the phantom's function can be restricted to a single process in question.

Today, much research is being directed to multi-modal image registration in order to take advantage of the complementary strengths of ultrasound, MRI and CT, and phantoms are being designed to validate this work. Not only must the structure be anatomically appropriate, and any mechanical characteristics prescribed, but the phantom must also be visible and resemble tissue in all of the desired modalities. Ongoing projects in our lab rely on the integration of ultrasound and MRI or x-ray images, and the validation of much of this work has required the construction of potentially deformable phantoms. PVA-C has played a key role in this research (Comeau *et al* 2000, Gobbi and Peters 2003, Surry *et al* 2003).

Methods

PVA liquid preparation

Commercial PVA powder was used to make our PVA liquids. Airvol Grade 165 PVA powder (Air Products and Chemicals, Inc; Allentown, PA) was chosen due to its very high level
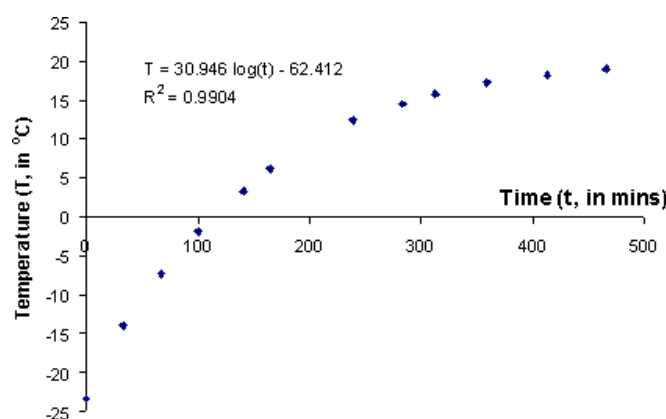
Figure 1. The rate of temperature increase in the PVA-C preparation freezer. Ambient is reached by 500 min.

of hydrolysis, at 99.3%. To make 10 wt% PVA liquid, 40 g of PVA powder and 360 g of de-ionized water were combined in a 1 litre Erlenmeyer flask, along with a magnetic stir bar. The weight of the flask and its contents were recorded. The mixture was stirred on a magnetic stir plate, to break any aggregates of powder. To fully dissolve the powder, the solution was brought to 121 °C in a steam autoclave for 30 min. The resulting clear gel was again stirred, for approximately 30 min, as it was cooled to room temperature. This cooling stage was important to ensure the formation of a homogeneous gel. When cool, the flask was weighed, and any loss in mass was replaced with de-ionized water, to ensure a consistent 10 wt% PVA solution. The solution was transferred to a storage container. Solutions can generally be kept for a maximum of two weeks, after which time biological contamination usually occurs.

PVA-cryogel

To form the PVA liquid solution into a solid phantom, the PVA liquid was first poured into the appropriate moulds. The liquid was allowed to rest for 12–24 h for air bubbles to rise to the surface and be removed. While resting at room temperature, the phantoms were kept well sealed, or in a humid environment, so that a dried skin would not form on the surface.

The standard freezing stage began at room temperature in a standard chest freezer. The phantoms were cooled from room temperature to −20 °C over 2 h and they were kept at this temperature for another 10 h, for a total freeze stage time of 12 h. During this time, a small fan circulated the air in the freezer. At the end of 12 h, the freezer was turned off, and it was allowed to slowly come back to room temperature over 8–9 h (figure 1). The thaw time depends on the size and number of the phantoms in the freezer. The freezer was kept at room temperature until the phantoms were entirely defrosted. They were then removed for use, or the freezer was turned back on to freeze, depending on the desired number of freeze–thaw cycles.

The PVA-C was then removed from the mould and stored in clean, de-ionized water, at 5 °C. With care, the phantoms can be kept indefinitely this way. In particular, replacing the water regularly helped us to extend the useful life of our phantoms.

PVA-C phantoms for characterization

In order to characterize this material in terms of its mechanical and imaging properties, we constructed cylindrical phantoms of different lengths. Acrylic tubing, with inner diameter of

63.5 mm and outer diameter of 76 mm, was cut into the following lengths: 20, 40, 60, 80 and 100 mm. These were glued to 76 mm thick acrylic sheet using an acrylic adhesive. They were further sealed using a silicone sealer around the seam.

10 wt% PVA liquid was poured into each mould, and allowed to rest for 24 h in a sealed water bath, with the water level about one quarter of the way up the sides of the shortest phantom. The bubbles that rose to the surface were scraped off and removed.

A complete set of phantoms, comprising one of each length, was processed through one freeze–thaw cycle, and another set for each of two, three and four freeze–thaw cycles. A final set was processed through a standard freezing stage, but was thawed in a water bath at a temperature depending on the size of the phantom. The temperature required for the bath was established from the principle that the amount of crystallization of PVA is determined by the thawing time (Hassan and Peppas 2000).

In order to produce homogeneous phantoms, the time required, Δt, to completely thaw the different sized samples from $-20\,^\circ\text{C}$ was kept constant. Since the amount of heat transfer, Q, was the same among all the phantoms (based on the temperature difference from frozen to complete thaw), the rate of heat transfer ($\dot{Q}_{\text{convection}}$) was also constant for each phantom:

$$\dot{Q}_{\text{convection}} = \frac{Q}{\Delta t} \tag{1}$$

$\dot{Q}_{\text{convection}}$ can also be written as a function of the surface area of a phantom, A, the heat transfer coefficient, h, and the temperatures, T, of the surface and the surrounding fluid:

$$\dot{Q}_{\text{convection}} = hA(T_{\text{surface}} - T_{\text{fluid}}). \tag{2}$$

The heat transfer coefficient is dependent on the material, and so was constant for all phantoms. The initial surface temperature (T_{surface} was estimated at $0\,^\circ\text{C}$) was also the same for all phantoms. The water bath temperature for the smallest phantom was chosen to be $20\,^\circ\text{C}$, which yielded a soft yet solid material at room temperature. The water bath temperatures for the other phantom sizes were calculated so that the heat transfer would be the same as for the smallest phantom (area, A_0) thawed in a $20\,^\circ\text{C}$ bath:

$$T_{\text{fluid}} = \frac{20A_0}{A}. \tag{3}$$

Thus, the bath temperatures were estimated for each phantom at 20, 30, 35, 40 and 45 °C for the smallest to the largest phantoms, respectively.

This challenge of achieving homogeneity in the thaw time was not as critical for the 12 h, in-freezer, thaw cycle since the convection fluid temperature (the air in the freezer) increased from $-20\,^\circ\text{C}$ to $20\,^\circ\text{C}$ concurrently with the phantoms, effectively minimizing the temperature difference at any given time for each phantom and decreasing the effect of the surface area differences.

Once the phantoms had undergone the physical cross-linking process, they were submerged in sealed containers filled with de-ionized water. This form of storage served to prevent any dehydration of the hydrogel polymer, while allowing the phantoms to reach equilibrium and undergo further crystallization by ageing. The effect of the ageing process was observed through measurement of phantom size throughout the first week of submersion, as seen in figure 2. Phantoms were stored for approximately 10 days before any experiments were conducted.

In some studies, it is necessary to construct phantoms with components that are distinguishable by their colour (for example, the breast biopsy phantom discussed below). For this purpose, we evaluated the effect of adding an enamel paint as a pigment to PVA-C on the material's imaging characteristics. PVA liquid, which had been prepared with the addition
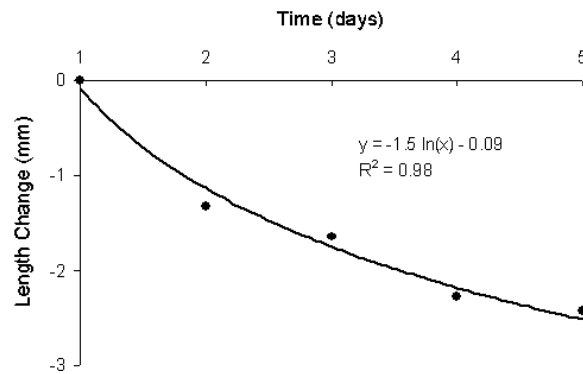
Figure 2. The change in phantom length, from the initial value after the freeze–thaw cycles were complete.

of 0.8% (by volume) enamel paint (Blue Metallic #1539; Testor Corp, Rockford, IL), was formed into another five sets of phantoms, in the same method as described above. The paint was stirred into the cooled liquid before it was poured into the moulds.

Characterization for ultrasound imaging: speed of sound measurements

The speed of sound can be described as the phase velocity of sound waves in the medium to be studied, and is also known as the 'sonic speed' or 'velocity of sound' (AIUM Technical Standards Committee 1995). This particular parameter is fundamental to the characterization of images acquired by ultrasound.

A simple fixed-path substitution technique was employed to determine the speed of sound in the cylindrical PVA-C phantoms. This method is the preferred standard for measuring small, intact phantoms, and involves the substitution of the sample for water over part of the signal path from the ultrasound transducer to the receiver (AIUM Technical Standards Committee 1995).

The speed of sound was determined by transmitting a pulse from a single crystal ultrasound transducer, through a water bath, to be received by another single crystal transducer, which was in line with the first. The transit time was measured for pure water, and compared with the transit time for the sound to travel the same distance, but with a sample placed in the signal path. De-ionized water was allowed to stand for at least 24 h at room temperature in the water bath before experimentation, to minimize the presence of small bubbles that might have interfered with the signal.

The sound wave was triggered by a Tektronix, PG 501 pulse generator (Beaverton, OR) with the following specifications: frequency of 3–8 MHz, depending on the experiment; period = 20 μs (50 kHz); pulse duration = 1 μs; pulse duration of 1 μs (approximately 2 cycles); output amplitude setting of 5 V. The pulse then travelled into a Wavetek Meterman, Model 148A function generator (Everett, WA), which constructed the desired sinusoidal waveform. The transmitted waveform was displayed by a Philips, Model PM 3365A oscilloscope, as was the waveform received by the second transducer. The on-screen cursors were used to measure the time difference between the leading edge of the transmitted pulse and the leading edge of the received pulse. The matching pulses were visualized by placing the ultrasound transducers face to face and then tracking the received pulse as the transducers were slowly separated to the experimental distances.

The cylindrical phantoms were placed near the centre of the signal path in the de-ionized water bath. The transducers were generally positioned at a distance that allowed the transmitted and received signals to be displayed simultaneously on the oscilloscope, since the distance is not otherwise imperative to the determination of the sonic velocity. The plane of the cylindrical face was oriented in a perpendicular attitude to the sonic signal, and the phantoms were constructed with the same diameter as the transducers, so that the pulse would travel through the approximate centre of the cylinder.

As a reference for transit time through a sample, the speed of sound in pure water is required. This is determined using the following equation (AIUM Technical Standards Committee 1995):

$$c_w = [1403 + 5T - 0.06T^2 + 3.0 \times 10^{-4}T^3] \text{ m s}^{-1} \tag{4}$$

where T is in $^\circ$C. Thus, having calculated this value, the exact distance between the transducer and receiver was determined by measuring the pulse transit time in a purely water medium according to the following equation:

$$d_{\text{transducers}} = c_w t_{\text{pulsetransit}}. \tag{5}$$

It was necessary to establish the transducer distance through calculations rather than by direct measurement, since the exact position of the piezoelectric crystal in the transducer casing could not be accurately determined.

Subsequently, the speed of sound in the sample, c_s, was calculated with the following equation using the speed of sound in water, c_w, and the depth of the phantom, d, which was measured using calipers.

$$c_s = \frac{c_w}{1 + \Delta t \frac{c_w}{d}}. \tag{6}$$

The challenge of this technique is the possible dependence of the speed of sound in a sample on the frequency of the waveform employed. Although the AIUM standards specify that the deviations in sound velocity are not significant in tissue-mimicking phantoms in the 1–3 MHz frequency range (AIUM Technical Standards Committee 1995), the majority of clinical ultrasound techniques require the use of 7.5 MHz. Consequently, measurements at a variety of frequencies, from 3 to 8 MHz were employed to better understand the relationship between frequency and velocity in these phantoms and to characterize this effect.

Characterization for ultrasound imaging: attenuation measurements

The attenuation of an ultrasound signal can be described as 'the fractional decrease in plane wave intensity per unit path length' (AIUM Technical Standards Committee 1995). Attenuation is a combination of both the scattering and absorption of the transmitted ultrasound waves and is a property that is characteristic of the composition and geometry of an object (Insana 1995).

The attenuation measurements were obtained using the same substitution technique and system set-up as the velocity measurements, with a few notable differences. The sinusoidal sound bursts required a duration of 10–20 cycles, as opposed to the two cycles that were employed with the velocity measurements. This was necessary to establish and effectively visualize the amplitude of the pulse.

It was also imperative that the receiving transducer be placed in the far field of the source transducer, at an axial distance that was at least a^2/λ, where a is the source transducer radius, and λ is the ultrasonic wavelength in water (AIUM Technical Standards Committee 1995). This far field requirement is due to the phase sensitivity of acoustic receivers, since near-field

conditions will result in destructive addition and consequent underestimation of the signal magnitude when the wave passes through an aberrating medium (Bamber 1998).

Therefore, given the source transducer diameter of 14 mm, a speed of sound of approximately 1484 m s^{-1} and a maximum frequency of 8 MHz, the minimum distance required, a^2/λ, was calculated as follows:

$$\lambda = \frac{c_w}{f} = \frac{1484 \text{ m s}^{-1}}{8 \times 10^6 \text{ s}^{-1}} = 1.855 \times 10^{-4} \text{ m} \tag{7}$$

$$\frac{a^2}{\lambda} = \frac{(7 \text{ mm})^2}{0.1855 \text{ mm}} = 264 \text{ mm}. \tag{8}$$

Unlike the methodology employed for the velocity of sound measurements, the originating pulse does not need to be compared to the received pulse directly, and only the amplitude of the transmitted signal and the received signal is required for calculation. The equation for the attenuation coefficient is given as

$$\alpha = \frac{20}{d} \log \frac{A_w}{A}, \tag{9}$$

where α was found for every frequency, d was the thickness of PVA-C in the beam, A_w was the attenuation of the signal through pure water and A was the attenuation of the signal with the PVA-C sample in the beam. The thickness of the PVA-C (d) was measured using digital calipers.

Characterization for MR imaging

All imaging was performed on a GE CVi 1.5T Clinical Scanner, using a quadrature birdcage head coil. The phantoms were placed together in a water bath, such that 'coronal' slices, as defined by the head coil orientation, showed a circular cross-section of each cylinder in the image. T1 values were obtained using a 2D inversion-prepared fast spin echo (FSE-IR) sequence with the following imaging parameters: echo time (TE) of 15 ms; repetition time (TR) of 5000 ms; successive inversion times (TI) of 50, 100, 200, 400, 800, 1600, 3200 ms; an echo train length of 4; a 256 × 192 matrix; 30 cm field of view (FOV); a 10 mm slice thickness; with a total imaging time of 28 min. T2 values were obtained through a 2D fast spin echo (FSE) sequence, with parameters as follows: a succession of TE values of 15, 30, 45, 60, 90, 120, 150, 195 ms; a TR of 5000 ms; an echo train length of 4; a 256 × 192 matrix; 30 cm × 20 cm FOV; a 10 mm slice thickness; and a total imaging time of 32 min; also, the pre-scan values were held constant throughout the acquisition of the FSE images. T1 and T2 values were obtained by post-processing using a nonlinear least-squares fitting routine to solve the FSE-IR and FSE signal equations for M_0, β, T1 and T2:

$$\text{SI(TI)} = M_0(1 - \beta \, e^{-\text{TI}/T_1}) \tag{10}$$

$$\text{SI(TE)} = M_0 \, e^{-\text{TE}/T_2}, \tag{11}$$

β was included to account for imperfect inversion pulses in the FSE-IR sequence and M_0 is the equilibrium magnetization within the voxel. After verifying experimentally that the methods yielded similar results, the FSE-IR and FSE sequences were chosen over the more conventional single-shot IR and SE approaches, to determine the T1 and T2 values, because of considerably reduced scan time (Deoni *et al* 2003). To account for imperfect inversion pulses, as well as coil sensitivity effects, the β term was included as a free parameter in the T1 fitting procedure.
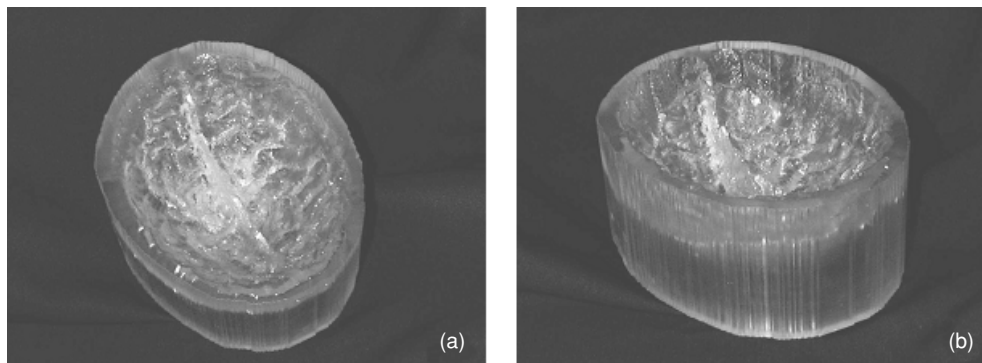
Figure 3. (a) The top view of a brain mould made by SLA from high quality MR image surface data. (b) The side view with support stand.

While FSE is not a true CPMG sequence, which could lead to inaccuracy in the T2 measurements resulting from the influence of stimulated echoes and T1 relaxation, the close agreement of measurements observed in our initial experiments (using FSE echo-train length of 4) demonstrated that these concerns had a negligible effect on our results.

Phantom applications

Homogeneous volume brain phantom. A human brain phantom, with surface features taken from a digital brain model is presented as an example of a simple homogeneous PVA-C phantom. The mould shown in figure 3 was created with a stereo-lithography apparatus (SLA), using a high quality 3D standard MR image (Holmes *et al* 1998) as input. The surface of the brain was extracted, and all structures below the cantho-meatal plane were discarded, to make an open-bowl shape for the mould. Filtering, and some manual processing, reduced the depth of the sulci, which would otherwise extend deeply into the PVA-C brain and cause difficulty in extracting the phantom from the mould. This surface was then coded in the appropriate digital format and transferred to a rapid prototyping facility (at the National Research Council of Canada's Integrated Manufacturing Technologies Institute, London, Canada) for production. The mould was created by laser deposition of plastic, layer by layer, starting at the bottom of the structure. The layer thickness was 0.10 mm, and the in-plane resolution of the laser was much less than the 1 mm^3 isotropic voxel resolution of the input image. 10 wt% PVA liquid was poured into the mould and it was kept in a humid environment for at least 24 h, or until all the bubbles had been expelled. There was no top surface to the mould, allowing for expansion during freezing. The phantom was frozen in a typical freeze–thaw cycle that was extended to a 48 h duration, to compensate for its large size. The phantom was carefully removed from the mould and kept in a water bath in a standard refrigerator.

Vessel phantoms. Walled vessel phantoms were constructed with PVA-C by making multi-component structures, which consisted of PVA-C volumes formed in layers. Arterial plaque in a vessel was simulated by constructing the simulated vessel in two phases. First, a mandrel in the shape of the stenosis (corresponding to the plaque volume) was matched with a tight-fitting sleeve with holes drilled where the stenosis cavity lay when inside the sleeve (figure 4(a)). With the sleeve on the mandrel, liquid PVA was injected into the stenosis cavity and this part was subjected to a single freeze–thaw cycle. A copper sleeve was used here to provide a faster thaw
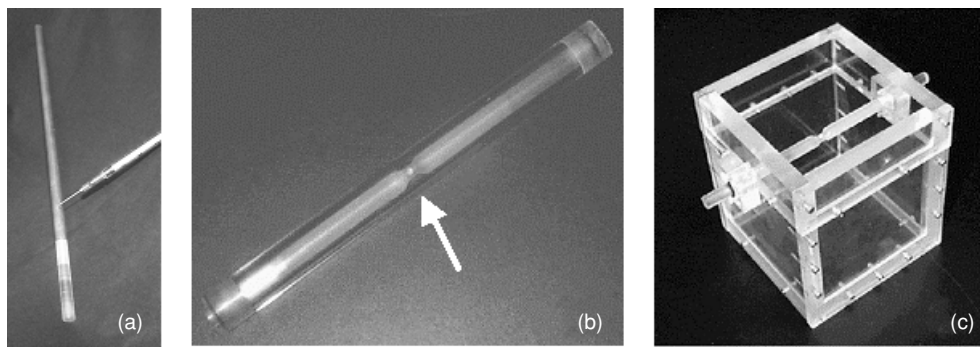
Figure 4. The three-stage process for a multi-volume stenosed vessel phantom. (a) Filling the tight-fitting sleeve over the mandrel to form the plaque. (b) The tube for making the vessel wall volume, with the stenosed mandrel centred with o-rings inside (this stenosis also had an ulceration, made by the bead of wax seen in the indentation at the arrow). (c) The final volume mould with the vessel mandrel centred in o-rings in the inlet and outlet moulds.

for the plaque volume and thus gave it properties more similar to the encasing vessel. When the PVA-C was solidified, the sleeve was carefully removed, leaving a small volume of formed PVA-C in the stenosis, as the plaque volume. The mandrel was then placed in a tube, with an inner diameter the same as the desired outer diameter of the wall of the vessel (figure 4(b)). To centre the mandrel, o-rings were fitted at each end, one inserted before and the other after filling the tube with PVA. After it was degassed and processed through one freeze–thaw cycle, the vessel wall mould was removed. The mandrel, with the PVA-C vessel on it, was placed in a mould box, centred through holes with o-rings and with the plaque volume oriented appropriately (figure 4(c)). The entire volume was then filled with PVA, and a lid was placed in contact with the surface. The phantom was degassed, then frozen and thawed for the last time. The 'plaque' was frozen and thawed a total of three times (including one 'quick' thaw), the vessel wall twice and the surrounding 'tissue' volume only once.

Breast biopsy phantoms. A phantom was designed for a biopsy experiment (Surry *et al* 2002), in which small embedded PVA-C cylinders, mimicking 'lesions', could be imaged with ultrasound prior to and after biopsy. Cylindrical 'lesions' were made by filling appropriately sized acrylic tubes with PVA, the largest being 16 mm in diameter, the smallest 1.6 mm. The PVA was coloured with enamel paint so that, when biopsied, the presence of coloured PVA-C in the sample would indicate a positive biopsy. After two freeze–thaw cycles, the cylinders of PVA-C were removed from the moulds and cut with a sharp knife into lengths equal to their diameter. A piece of nylon thread was sewn through the surface of the lesion and then threaded up through a 1.5 mm diameter hypodermic tube. These stainless steel tubes had been glued into a flat plate that was part of the lid of the phantom, so that the lesions could be suspended in the PVA volume. The container for the tissue mimic volume was filled with PVA and the lid placed on top with the lesions hanging down at the same depth and fixed with respect to each other. After the PVA-C had been gelled, the threads were cut away from the outside so that the lid, with the embedded hypodermic tubes, could be lifted away from the phantom. The tubes would thus be removed from the phantom, leaving threads emerging from vertical wells with the same diameter as the tubes. The phantom was then imaged upside-down, so that these wells were behind the lesions and any effects from the voids or the increased thaw time caused by the tubing would be outside of the volume of interest.

For a more realistic breast phantom, in both tactility and when viewing with ultrasound, a chicken breast phantom, with embedded PVA-C lesions was developed (Smith *et al* 2002). This tissue-mimicking material provided the resilience and inhomogeneities found in human breast tissue, and thus provides an approximation of tactile feedback during biopsy needle insertion. To create the lesions, the PVA liquid was inserted with a syringe into a series of acrylic tubes with a 3.2 mm inner diameter (51.2 mm long, and 9.6 mm outer diameter), and frozen as above, but thawed at room temperature (in under 1 h). The strands were only very slightly gelled, being able to support their cylindrical shape, but would flatten with gentle pressure. However, these strands were not fragile, and required a sharp edge to cut them. Using razor blades, the strands were cut into short cylinders of approximately 3.2 mm in length. The material used for the surrounding tissue mimic in these phantoms was fresh, skinned and boned chicken breast. Lesions were inserted into small slots cut into the chicken breasts. Twelve lesions were placed in the top surface of each of two chicken breasts. An additional 12 lesions were placed in the underside of a third breast. The three chicken breasts were then stacked, top surfaces upwards, and the breast with the lesions on its underside made the top layer. The lesions in the top breast were then sufficiently deep to be outside the near-field of the US beam, and the slits in which they were located were kept closed by pressure between successive breast layers. The stacked breasts were placed on a foam plate and the chicken breasts were sewn together in a blanket stitched using butcher's twine through all the layers and around the entire edge of the phantom. Mesh netting (5 mm circular nylon mesh) was wrapped around the stitched edge of the phantom to provide stability.

Results and discussion

Characterization for ultrasound imaging

After four separate trials were conducted for acoustic velocity at varying frequencies, it was found that there was no discernable correlation between the frequency and velocity. There is controversy about the relationship between acoustic velocity and frequency in the literature, and because there was no trend found in this study, we report only acoustic velocity as it changes with freeze–thaw cycles and additives (Lees and Klopholz 1992, Kohles 1996). The speed of sound in 10% PVA-C, with and without 0.8% enamel paint, is shown in figure 5. There is a clear increase in speed of sound with number of freeze–thaw cycles. The addition of enamel paint also does not seem to affect the speed of sound in the material, except with a single freeze–thaw cycle. The standard deviation in each point is less than 0.5% (3–8 m s^{-1}). Note that the four times frozen sample has speed of sound values close to that assumed by clinical ultrasound scanners (1540 m s^{-1}). However, with accurate knowledge of the speed of sound in a sample, precise measurements can be made by compensating for differences in speed of sound.

Figure 6 shows the attenuation coefficients for 10% PVA with and without 0.8% enamel paint added for one through four freeze–thaw cycles. In both cases, the attenuation coefficient (in dB cm^{-1}) increases with the number of freeze–thaw cycles. The figure displays the coefficients as dependent on frequency, for clarity. For plain PVA-C, the frequency-independent attenuation coefficients were 0.075, 0.12, 0.21 and 0.22 dB (cm MHz)$^{-1}$, for one through four freeze–thaw cycles, respectively (standard deviations in these values are 10% or less). Attenuation in human tissue varies widely, with reported ranges as low as 0.3–0.5 dB (cm MHz)$^{-1}$, as opposed to the traditional rule of 1 dB (cm MHz)$^{-1}$ (Insana 1995). These values are considerably higher than those achieved with PVA-C, and present the most significant drawback to this material in ultrasound imaging.
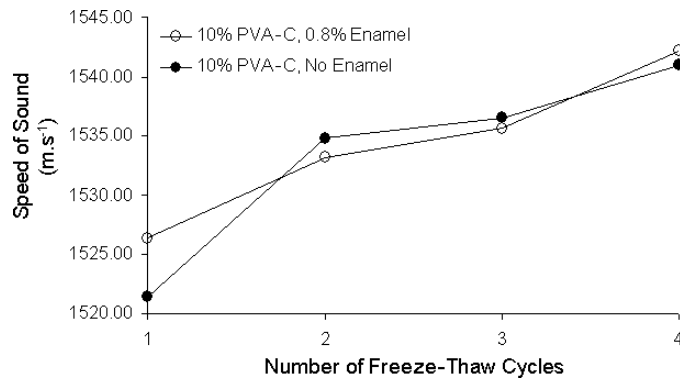
Figure 5. The speed of sound in 10% PVA-C, with and without 0.8% enamel paint added, as it changes with the number of freeze–thaw cycles.
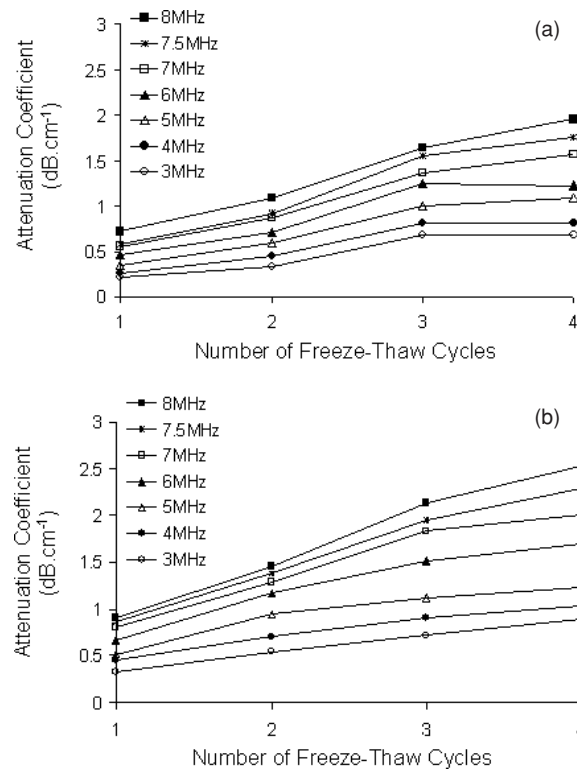

Figure 6. The attenuation coefficients for 10% PVA-C, (a) with and (b) without 0.8% enamel paint. The coefficients are quoted in dB cm^{-1}, for each frequency, for clarity.

For PVA-C with added enamel (figure 6(b)), the attenuation coefficients are higher, with values ranging from 0.33 to 2.52 dB cm^{-1}. The frequency-independent attenuation coefficients, in this case, were found to be 0.11, 0.18, 0.25 and 0.28 dB (cm MHz)$^{-1}$, for one through four freeze–thaw cycles, respectively (standard deviations in these values are 10% or less).
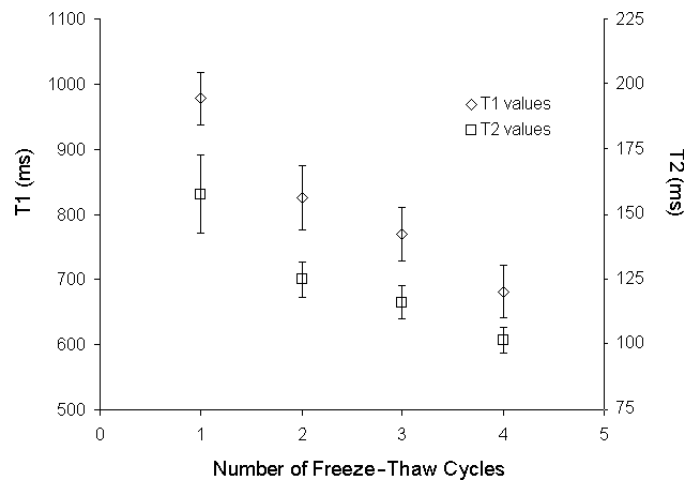
Figure 7. MR relaxation coefficients, T1 and T2, for 10% PVA-C.
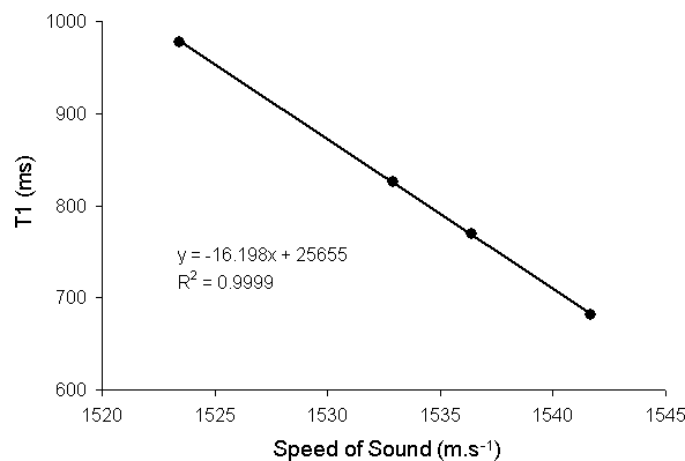

Figure 8. A linear relationship was found between T1 and speed of sound in 10% PVA-C.

Characterization for MR imaging

T1 and T2 values for 10% PVA-C without enamel paint are shown in figure 7. T1 values decreased with the number of freeze–thaw cycles, from 1034 to 718 ms. T2 values also decreased with freeze–thaw cycles. The drop from one freeze–thaw cycle (175 ms) to two freeze–thaw cycles was 38 ms, but from two to three freeze–thaw cycles, was only 10 ms. The difference between one freeze–thaw cycle and four freeze–thaw cycles was 67 ms.

Figure 8 shows a linear trend between speed of sound and T1 values. A similar relationship was not found with T2. The T1 correlation relationship could be useful in confirming the speed of sound values in irregularly shaped PVA-C phantom structures.

Phantom applications

3D ultrasound and MR images of the brain phantom are shown in figure 9. The central sulcus and surface morphology can be clearly seen. The MR image of the brain phantom
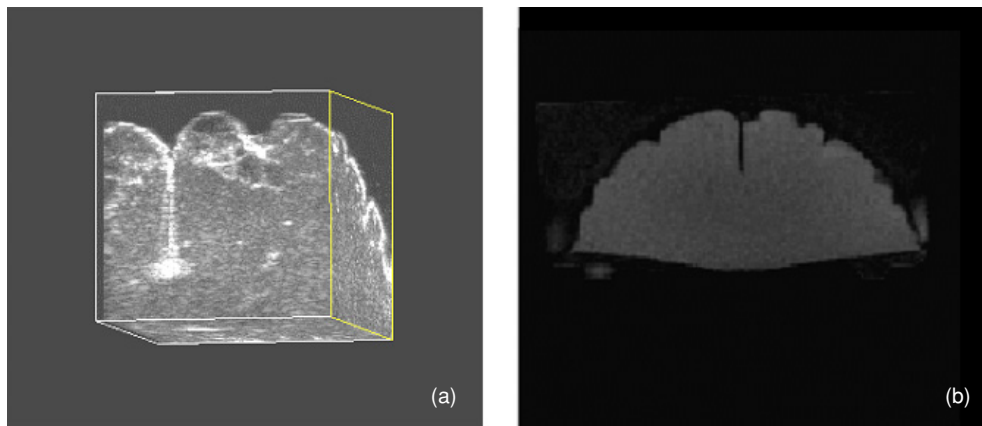
Figure 9. (a) A 3D US image of the PVA-C brain phantom, showing the central sulcus. (b) Coronal slice of the same phantom in MRI.
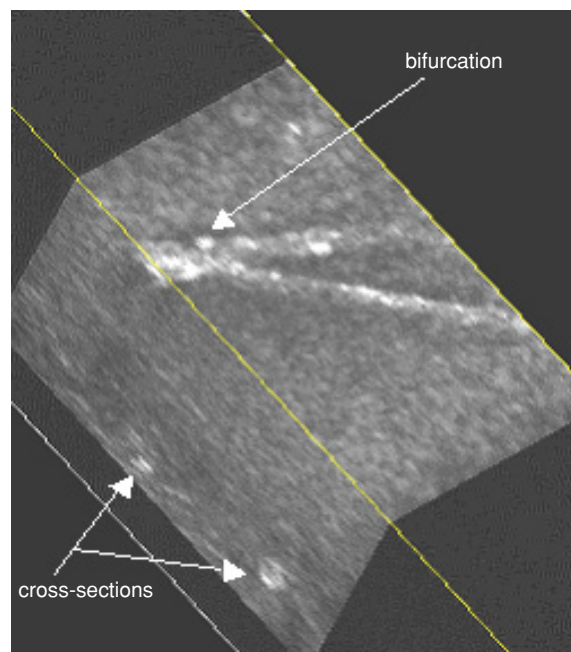

Figure 10. Three-dimensional US image of a phantom containing two branched vessels. The front face of the image shows cross-sections of the outlet vessels of a branched pair. The top surface shows the plane of the second branched vessel.

was compared with the source MR image, and a ±0.7 mm error was found in the registration of homologous points on the cortical surface (overall scaling factor for the fit was 1.044) (Surry and Peters 2001). This phantom has been used in dual modality image guided surgery research, as described by Gobbi and Peters (2002).

Vessel phantoms can be seen in figures 10 and 11. The first is a bifurcated vessel phantom with a homogeneous volume. The bifurcation was made by applying a weak adhesive between
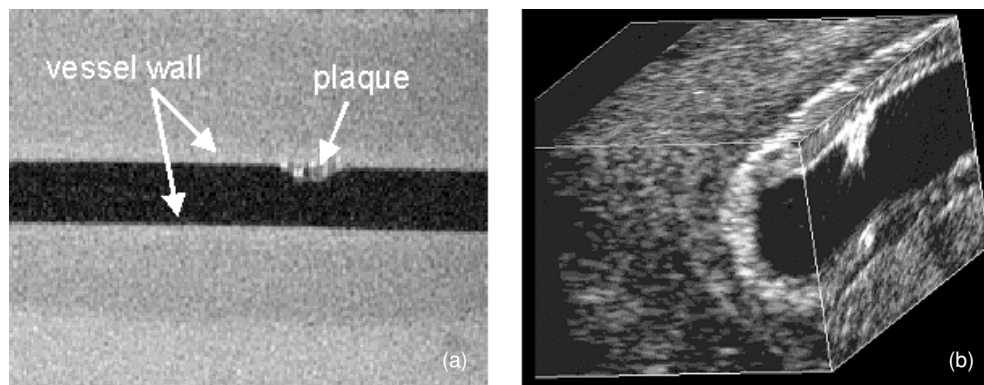
Figure 11. The multi-volume stenosed vessel phantom, made with the moulds of figure 6, shown in cross-section in (a) MRI and (b) ultrasound. The different layers are clearly visible in both modalities.
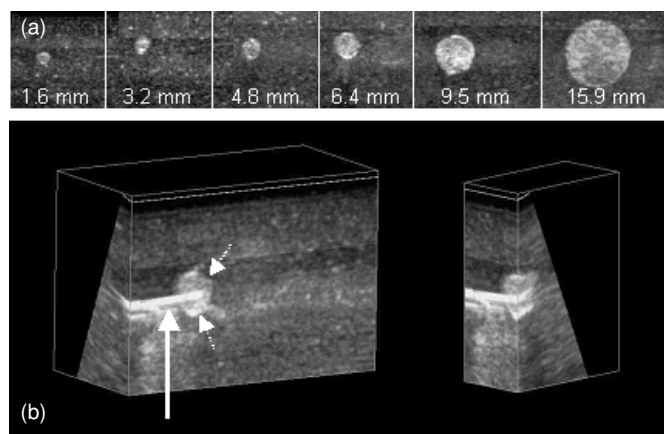

Figure 12. A series of breast biopsy phantoms were made, with three freeze–thaw cycle cylindrical 'lesions' embedded in surrounding tissue made from one freeze–thaw cycle PVA-C. (a) This series of ultrasound images shows a cross-sectional plane of all lesion sizes, from 1.6 mm to 15.9 mm, in ultrasound. (b) The lesion targeting phantom in 3D US. The biopsy needle (solid arrow) is in place for sampling the PVA-C lesion (dotted arrows). The right-hand image shows how the biopsy can be confirmed using another plane in the 3D US image.

the three branches of the vessel mould, which could be broken by twisting each branch and the parts were pulled out separately. The second type of vessel phantom demonstrated the use of freeze–thaw cycles to create multi-volume structures. The plaque, vessel wall and surrounding tissues were all visible in both US and MRI. These structures were subjected to three, two and one freeze–thaw cycles, respectively.

Another phantom which made use of multiple freeze–thaw cycles was a breast biopsy phantom, shown in figure 12. This was one of a series of phantoms that provided targets of known size and shape, at a fixed depth in ultrasound, and at a fixed distance from the insertion point of the needle. The six target sizes are shown in cross-section in the figure. The lesions were frozen and thawed three times, compared to the once-frozen background, and
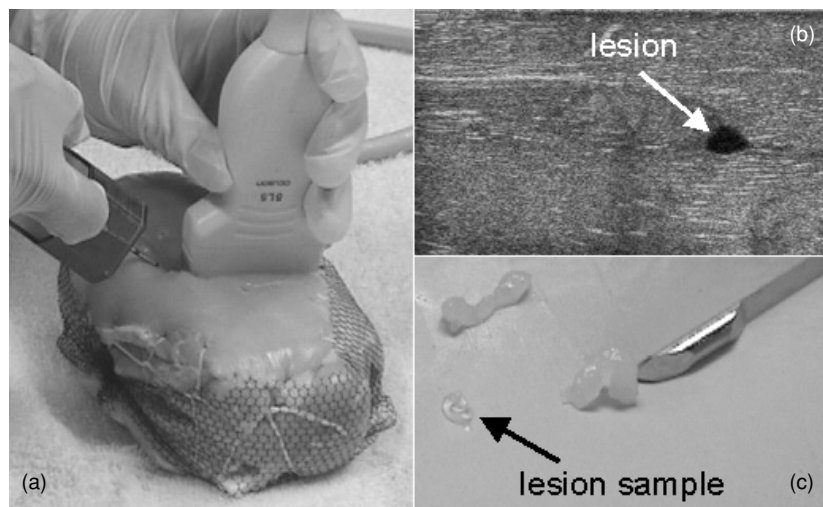
Figure 13. (a) The chicken breast biopsy phantom, in use. (b) The 3.2 mm diameter, fast-thaw PVA-C 'lesion' was embedded in fresh chicken breast and is shown in 2D ultrasound. (c) The 'lesion' material was clearly distinguishable from the surrounding chicken tissue in the biopsy sample. The needle was about 2 mm in diameter.

were coloured with enamel paint, to distinguish them in a biopsy sample. The phantoms were used in a biopsy accuracy study, described in Surry *et al* (2002).

A final phantom (figure 13) combined PVA-C with animal tissue, for a different breast biopsy phantom study. These phantoms provided a means to compare biopsy techniques, because they were similar in both tactility and ultrasound structure to human breast tissue (Smith *et al* 2002). Here, a targeting task, rather than an identification task was evaluated. Thus, we chose a target which was clearly visible against the chicken tissue background. The fast-thawed PVA-C 'lesions' provided cyst-like masses that were clearly hypoechoic in the US images. This PVA-C preparation was also necessary to have a target that was sufficiently soft for biopsy. One full freeze–thaw cycle made PVA-C lesions that slid out of the way as the needle approached, but the fast-thaw PVA-C allowed the material to be easily penetrated with the needle.

General comments

There are some general comments that can be made about PVA-C phantom construction and use, which may be useful for other researchers wishing to investigate this material. The first is that the phantoms described above all used 10% PVA prepared PVA-C. Its low viscosity at room temperature and low shrinkage post-freeze–thaw cycle made it the most versatile for the different phantoms, particularly when filling small diameter tubes, and for maintaining its shape after forming.

Support for internal structures may be constructed so that they can be removed after forming, or be such that they would not interfere with the volume of interest when imaging. Fine threads for suspension are useful and unobtrusive. Posts can be removed, but leave cylindrical voids. Care should also be taken when choosing to use metal in the mould, due to its high thermal conductivity. Local rapid thawing around a metal part has produced imaging artefacts in an otherwise homogeneous phantom. These are all considerations

to be made in the phantom design within the particular constraints of an experimental problem.

Included structures can be used for reference marker points, and may be constructed of PVA-C, to benefit from its multi-modal properties, or of a different material, like plastic pellets or pockets of MR contrast agents. It was found, however, that any soluble liquid would not stay localized, but would diffuse through the phantom, as found using gadolinium (Gordon *et al* 1999).

Conclusions

Poly(vinyl alcohol)-cryogel (PVA-C) is a useful phantom material, with well described ultrasound and MR characteristics. Depending on preparation, the velocity of sound in PVA-C was found to be 1520–1540 m s^{-1}, which is well within the typical range for tissue (Robinson *et al* 1991). T1 values obtained through MR imaging studies were also found to be similar to values for grey and white matter and muscle, but T2 values were higher, suggesting that this material may be appropriate for T1-weighted imaging studies (Bushberg *et al* 1994). Interestingly, a linear relationship was also found between velocity of sound and T1 values, which could be used as a straightforward method for confirming the speed of sound in phantoms. This behaviour recalls our earlier work on the temperature memory characteristic of PVA-C, which related T1 values to the temperature to which a PVA-C sample had been previously exposed (Lukas *et al* 2001).

The phantoms used in the ultrasound and MR characterization study were prepared in a careful and controlled manner, with respect to the freeze and thaw times. However, for larger or inhomogeneous phantoms there may be an unknown or varying times for freeze and thaw, resulting in unknown or inhomogeneous characteristics across the volume. An MR T1 map may be able to accurately characterize the speed of sound across a phantom, such that accurate measurements may be made from an ultrasound image.

The ultrasound attenuation coefficient found for PVA-C presents the main disadvantage for this material as a tissue-mimicking material. The coefficients were found to be 0.075–0.28 dB (cm MHz)$^{-1}$, compared to the rule of thumb of 1 dB (cm MHz)$^{-1}$ for tissue. This does not affect the accuracy of reading ultrasound images, and can be compensated for by adjusting the gain on the ultrasound machine; however, it is not a direct substitute for tissue. The range of attenuation coefficients is sufficient to allow for multi-volume phantoms with volumes distinguishable from each other, due to their attenuation differences.

Brain, vessel and breast biopsy phantoms have been successfully developed using PVA-C. Most of these phantoms have been used in published research. The surface morphology of the brain phantom was useful in a multi-modality study (Gobbi and Peters 2002, Surry and Peters 2001), and multi-volume phantoms were used in biopsy accuracy studies (Surry *et al* 2002). This demonstrated that small, regularly or irregularly shaped volumes that are frozen a different number of times than the surrounding tissue could be easily targeted with ultrasound or MR, for segmentation or biopsy.

Acknowledgments

References

AIUM Technical Standards Committee 1995 Methods for specifying acoustic properties of tissue mimicking phantoms and objects (Laurel, MD: American Institute of Ultrasound in Medicine)

Bamber J C 1998 Ultrasonic properties of tissues *Ultrasound in Medicine* ed F A Duck, A C Baker and H C Starritt (Bristol: Institute of Physics Publishing)

Blechinger J C, Madsen E L and Frank G R 1988 Tissue-mimicking gelatin-agar gels for use in magnetic resonance imaging phantoms *Med. Phys.* **15** 629–36

Bushberg J T, Seibert J A, Leidholt E M and Boone J M 1994 *The Essential Physics of Medical Imaging* (Hagerstown, MD: Lippincott Williams and Wilkins) p 308

Cha W I, Hyon S H and Ikada Y 1993 Microstructure of poly(vinyl alcohol) hydrogels investigated with differential scanning calorimetry *Makromol. Chem.* **194** 2433–41

Chu K C, Jordan K J, Battista J J, Van Dyk J and Rutt B K 2000 Polyvinyl alcohol-Fricke hydrogel and cryogel: two new gel dosimetry systems with low Fe^{3+} diffusion *Phys. Med. Biol.* **45** 955–69

Chu K C and Rutt B K 1997 Polyvinyl alcohol cryogel: an ideal phantom material for MR studies of arterial flow and elasticity *Magn. Reson. Med.* **37** 314–9

Comeau R M, Sadikot A F, Fenster A and Peters T M 2000 Intraoperative ultrasound for guidance and tissue shift correction in image-guided neurosurgery *Med. Phys.* **27** 787–800

De Korte C L, Cespedes E I, Van Der Steen A F W, Norder B and TeHijenhuis K 1997 Elastic and acoustic properties of vessel mimicking material for elasticity imaging *Ultrason. Imaging* **19** 112–26

Deoni S L C, Rutt B K and Peters T M 2003 Rapid combined T1 and T2 mapping using gradient recalled acquisition in the steady state *Magn. Reson. Med.* **49** 515–26

Dyson R W 1998 *Specialty Polymers* 2nd edn (London: Blackie Academic & Professional) pp 78–85

Gobbi D G and Peters T M 2002 Interactive intra-operative 3D ultrasound reconstruction and visualization *Lecture Notes in Computer Science* vol 2489 *Proc. MICCAI 2002 (Tokyo, 25–28 Sept. 2002)* ed T Dohi and R Kikinis (Heidelberg: Springer) pp 156–63

Gobbi D G and Peters T M 2003 Generalized 3D nonlinear transformations for medical imaging: an object-oriented implementation in VTK *Comput. Med. Imaging Graph* **27** 255–65

Gordon M J, Chu K C, Margaritis A, Martin A J, Ethier C R and Rutt B K 1999 Measurement of Gd-DTPA diffusion through PVA hydrogel using a novel magnetic resonance imaging method *Biotechnol. Bioeng.* **65** 459–67

Hassan C M and Peppas N A 2000 Structure and applications of poly(vinyl alcohol) hydrogels produced by conventional crosslinking or by freezing/thawing methods *Adv. Polym. Sci.* **153** 37–65

Holmes C J, Hoge R, Collins L, Woods R, Toga A W and Evans A C 1998 Enhancement of MR images using registration for signal averaging *J. Comput. Assist. Tomogr.* **22** 324–33

Insana M F 1995 Sound attenuation in tissue *Medical CT & Ultrasound* ed L W Goldman and J B Fowlkes (Madison, WI: Advanced Medical Publishing)

Kohles S S 1996 Minimal dependence of ultrasonic propagation velocity on frequency *Ultrasound Med. Biol.* **22** 1297–8

Lees S and Klopholz D Z 1992 Sonic velocity and attenuation in wet compact cow femur for the frequency range 5 to 100 MHz *Ultrasound Med. Biol.* **18** 303–8

Lozinsky V I, Vainerman E S, Domotenko L V, Mamtsis A M, Titova E F, Belavtseva E M and Rogozhin S V 1986 Study of cryostructurization of polymer systems VII. Structure formation under freezing of poly(vinyl alcohol) aqueous solutions *Colloid Polym. Sci.* **264** 19–24

Lukas L A, Surry K J M and Peters T M 2001 Temperature dosimetry using MR relaxation characteristics of poly(vinyl alcohol) cryogel (PVA-C) *Magn. Reson. Med.* **46** 1006–13

Madsen E L, Zagzebski J A, Banjavie R A and Jutila R E 1978 Tissue mimicking materials for ultrasound phantoms *Med. Phys.* **5** 391–4

Mano I, Goshima H, Nambu M and Iio M 1986 New polyvinyl alcohol gel material for MRI phantoms *Magn. Reson. Med.* **3** 921–6

Mitchell M D, Kundel H L, Axel L and Joseph P M 1986 Agarose as a tissue equivalent phantom material for NMR imaging *Magn. Reson. Imaging* **4** 263–6

Mori Y, Tokura H and Yoshikawa M 1997 Properties of hydrogels synthesized by freezing and thawing aqueous polyvinyl alcohol solution and their applications *J. Mater. Sci.* **32** 491–6

Nagura M, Hamano T and Ishikawa H 1989 Structure of poly(vinyl alcohol) hydrogel prepared by repeated freezing and melting *Polymer* **30** 762–5

Nagura M and Ishikawa H 1984 State of water in highly elastic poly(vinyl alcohol) hydrogel prepared by repeated freezing and melting *Polym. Commun.* **25** 313–4

Peppas N A 1975 Turbidimetric studies of aqueous poly(vinyl alcohol) solutions *Makromol. Chem.* **176** 3433–40

Rickey D W, Picot PA, Christopher D A and Fenster A 1995 A wall-less vessel phantom for Doppler ultrasound studies *Ultrasound Med. Biol.* **21** 1163–76

Robinson D E, Ophir J, Wilson L S and Chen C F 1991 Pulse-echo ultrasound speed measurements: Progress and prospects *Ultrasound Med. Biol.* **17** 633–46

Ryan L K and Foster F S 1997 Tissue equivalent vessel phantoms for intravascular ultrasound *Ultrasound Med. Biol.* **23** 261–73

Smith W L, Surry K J M, Kumar A, McCurdy L, Downey D B and Fenster A 2002 Comparison of core needle breast biopsy techniques: Freehand versus three-dimensional US guidance *Acad. Radiol.* **9** 541–50

Stauffer S R and Peppas N A 1992 Poly(vinyl alcohol) hydrogels prepared by freezing-thawing cyclic processing *Polymer* **33** 3932–6

Surry K J M, Mills G R, Downey D B and Fenster A 2003 Image guided breast biopsy using 3D ultrasound and stereotactic mammography *Proc. SPIE* **5029** 376–83

Surry K J M and Peters T M 2001 A PVA-C brain phantom derived from a high quality 3D MR data set *Lecture Notes in Computer Science* vol 2208 *Proc. MICCAI 2001 (Utrecht 14–17 Oct. 2001)* ed W J Niessen and M A Viergever and (Heidelberg: Springer) pp 1149–50

Surry K J M, Smith W L, Campbell L J, Mills G R, Downey D B and Fenster A 2002 The development and evaluation of a three-dimensional ultrasound-guided breast biopsy apparatus *Med. Image Anal.* **6** 301–12

Watase M 1989 Effect of the degree of saponification on the rheological and thermal properties of poly(vinyl alcohol) gels *Makromol. Chem.* **190** 155–63